Analysis and Experiment of Flow Field in Sugarcane Leaf Cutting and Returning Machine

Haiyan Dai[1], Yuxing Wang[1]* , Fujun Wen[1] and Yanqin Tang[1]

1 Collage of Engineering, South China Agricultural University, 483 Wushan road, Tianhe district , Guangzhou, 510642, China.
Email: scauwyx@scau.edu.cn

Abstract. In order to improve the sugarcane leaves cutting effect of electric sugarcane leaves returning machine, the sugarcane cutting process is modeled and simulated by ANSYS/LS-DYNA software. It shown that in the double-support cutting mode, the cutter roller ensures the multi-layer sugarcane leaves were cut at the rotate speed of 800r/min. During the cutting process of sugarcane leaves, the stress is mainly concentrated at the incision, and the sugarcane leaves on the side of the blade are subjected to greater stress. The smaller the distance between the rotary blade and the fixed blade of the same combination, the easier the sugar cane leaves are cut off. In the cutting test of sugarcane leaves, the cutting rate was 91.47%, which echoed the simulation results, indicating that modeling and simulation have reference value.

1. Introduction

Sugarcane is a kind of perennial plant. In the harvest season, a large number of sugarcane leaves are left in the field. They must be processed for their large length and high toughness; otherwise, they will affect the subsequent mechanized farming seriously. Burning on the spot is the simplest and cheapest way to process the sugarcane leaves, but the burning is likely to cause serious problems such as air pollution, nutrient loss, fire and traffic accidents, and so on [1]. The most effective way to solve the problems is mechanized sugarcane leaves returning to the field. Since the 80s of last century, research on mechanized sugarcane leaves returning to field technology have been conducted in China. 3SY-120, 3SY-140 and 3SY-180 types of sugarcane leaf crushing machines are designed and manufactured by Guangxi Agricultural Machinery Research Institute [2]. 1GYFH, 1GYF-120, 1GYF-150, 1GYF-200 and GYF-250 types of sugarcane leaf crushing and returning machines are developed by the Institute of Agricultural Machinery Research Institute of Chinese Academy of Tropical Agricultural Sciences [3]. The above research mainly focuses on the design and test of the whole structure of sugarcane leaf machine. Although the types of machine have a good effect on the pulverization of sugarcane leaves, the structure is complex, and needs a large amount of power which would cause large weight. It has a serious compaction effect on the soil and affects the growth of sugarcane perennial roots. To solve this problem, research on remote-controlled self-propelled sugarcane leaf cutting and returning machine are conducted in South China Agricultural University. Flexible knives to cut the sugarcane leaves into pieces are used on the machine. Low power, light weight and having nice operating environment are the advantages of the machine, but it is found that the cutting effect of sugarcane leaves is not ideal for the winding caused by the self-excited airflow through experiments. In order to reduce the winding of sugarcane leaves and seek the best way to work without changing the structure, the internal flow field under the different working modes of the machine was analyzed by using the LS-DYNA software and the arbitrary Lagrange-Euler method (ALE) [4-9]. Finally, the wind speed test and the high speed photography [10-15] were carried out to verify the accuracy of the simulation results.

1.1. The Structure of The Whole Machine and Its Working Principle and the Structure of Sugarcane Leaf Returning Machine and Its Working Principle

The sugarcane leaf cutting and returning machine adopts crawler type chassis, and its structure is shown in Figure 1. It is mainly composed of battery, walking mechanism, cutting device, frame, dome and so on. The walking mechanism mainly consists of walking motor, driving wheel, caterpillar track, tensioning wheel and driven wheel. There are two walking motors, which are installed on the side of the left and right wheels to drive the wheels. The cutting system includes working motor, belt 1, belt 2, belt wheel 1, belt wheel 2, main knife roller, driven knife roller, knife plates and flexible knives. The outer end of the working motor is equipped with a belt wheel, each of which is installed with two knife plates, and the flexible knife is consolidated on the knife roller through the knife plate.

In the process of the returning machine, the electric energy of the battery can be distributed to supply the walking motor and the working motor. The size and direction of the walking motor's speed can be adjusted by the hand-held remote controller, and the forward, backward, left turn and right turn motions of the returning machine can be realized. When the two motor is moving clockwise at the same speed, the returning machine is straight forward; when the two walking motor is moving anti-clockwise at the same speed, it is straight backward; when the rotational speed of the left motor is less than the right speed, it is turned left movement; conversely, right turn movement.

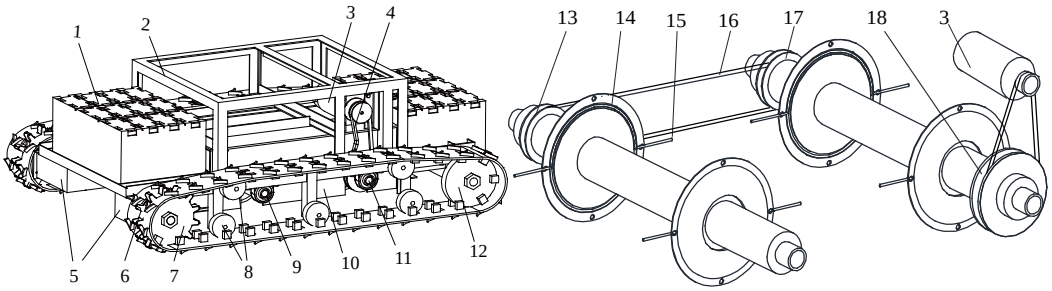

a. The structure of the returning machine b. The structure of the cutting system

1. Battery 2. Frame 3.Working motor 4. Belt 1 5. Walking motor 6. caterpillar track
7. Driving wheel 8. Tensioner pulley 9. The driven knife roller 10.Dome
11. The main knife roller 12. Driven wheel 13. Pulley 1 14. Knife plate
15. Flexible knife 16. Belt 2 17. Pulley 2 18. Pulley 3

Figure1. Engineering Drawing of Sugarcane Leaf Cutting and Returning Machine

When the working motor is started, the motor passes the power to the main knife roller through the belt wheel and the belt, and the main knife roller passes the power to the driven knife roller through the belt driving. The knife plates mounted on the knife rollers rotate at high speed. It is used to drive the flexible knife to beat sugarcane leaves, thus cutting off them. In order not to damage the ratoon, the cutting knife is made of flexible PA66 material. During the working process, the cutting device and the dome form a common working space.

1.1.1. Whole Machine Parameter

The length of sugarcane leaf is generally 80~150cm, and the width is about 2~8cm [16]. According to agronomic requirements, if the length of the leaves is less than 25cm, it can get good effect of sugarcane leaf returning to field, and achieve reutilization of resources. Based on the design requirements, the main structural and technical parameters of the machine are shown in Table 1.

Table 1. Structure and Technical Parameters of Sugarcane Leaf Cutting and Returning Machine

structure and technical parameters	design value
shape size (long × width×height)	1186×800×404
rated power of walking motor/kw	350
rated power of working motor/kw	400
curb weight/kg	≤150
the rotating speed of the main roller / $r \cdot min^{-1}$	3000
the rotating speed of the driven roller/$r \cdot min^{-1}$	2800
working speed/ $m \cdot s^{-1}$	0.4
operation width/mm	800
number of knife rollers	2
number of flexible knifes	4
number of batteries	24

2. Simulation Model and Related Settings

2.1. Basic Assumptions of Simulation

1) Assuming that the machine walks without wind, the speed of the returning machine is 0.4m/s, then the wind caused by travel is neglected in initial state.

2) The self-excited wind field generated by the rotary motion of the flexible knife has little influence on the ground, the knife roller and the dome, so the three parts are regarded as a rigid body.

3) In reality, the volume of the ground and air is endless, but the surface and air outside the dome have little influence. Therefore, only the finite volume that surrounds the whole dome, the knife rollers and the flexible knives can be considered for the air model.

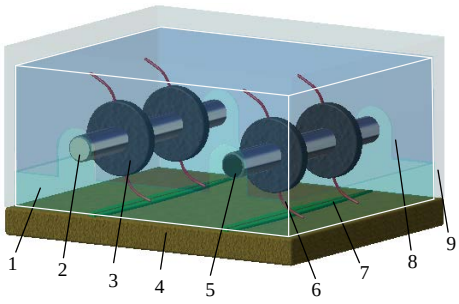

1. Air outlet 2. The main knife roller 3.Knife dish 4. Ground

5. Driven Knife roller 6. Flexible knife 7. Sugarcane leaf 8. Dome 9.Air

Figure 2. Simulation Model

The simplified structure is shown in Figure 2. The dome is located outside of the two knife rollers, wrapping the cutting device, the distance is 50mm from the ground to the bottom of the dome, and the gap is the air outlet of the self-excited wind field. The finite volume which is enclosed by the dome, the floor, the knife rollers and the flexible knives, is the volume corresponding to the self-excited wind field.

2.2. The Establishment of Finite Element Model

2.2.1. The Knife Roller, Dome and Ground Material Model

According to the assumptions of the model, the structural components and fluid inside the dome are mainly considered, the material model of knife roller and knife plate adopts rigid material model

MAT_RIGID, the type is set to solid164 unit with a density of 7820 kg/m^3, a modulus of elasticity of 207GPa, and a Poisson's ratio of 0.28. Flexible knives use nylon PA66 material, select solid164 unit, set material density is 1400kg/m^3, shear modulus is 3.01GPa. The dome model is set to shell163 element with a thickness of 2mm and 304 stainless steel with a density of 8000 kg/m^3, a modulus of elasticity of 210GPa, and a Poisson ratio of 0.3.

2.2.2. Air Material Model

The air is regarded as an ideal gas with a density of 1.25 kg/m^3 and a dynamic viscosity coefficient of 1.7456×10^5 N·s/m^2. The equation of state is defined as a linear polynomial; the air state equation is that:

$$p = C_0 + C_1\mu + C_2\mu^2 + C_3\mu^3 + \left(C_4 + C_5\mu + C_6\mu^2\right)e_{ipv0} \tag{1}$$

The C0~C6 are the constant coefficients, and eipv0 is the initial internal energy. Because it is an ideal gas, there is an initial pressure, but no initial pressure input in the parameters of the equation of state. It should be converted into the initial internal energy input, and the initial internal energy is input as follows:

$$P = (\gamma - 1)\frac{1}{v_{rel}}e_{ipv0} \tag{2}$$

The γ is the specific heat of the gas, the value is 1.4 kJ/(m^3·℃), the relative volume is 1, and the P is the gas pressure. The initial internal energy e_{ipv0} can be calculated to be 2.5331×10^5 J. To ensure the calculation progress, and to reduce the calculation time and divide the air grid, the number of grid units is controlled by line size, and the size of the air mesh in contact with the flexible knife is smaller and the grid is much denser. In order to prevent leakage, the mesh density of the dome is larger than the air.

2.2.3. Definition of Fluid-Solid Coupling and Setting of Initial Conditions

After establishing the simulation model, we set up the related constraints and contact conditions, add the fluid-solid coupling keywords, set up the air as the main component; combine the rigid body such as the ground, the dome, the knife rollers, the knife plate and the flexible knives, set them into the subordinate parts, and use the penalty function method to get the fluid-solid coupling.

In order to simulate the infinite volume of air and ground, the boundary between the air and the ground model is set to the non-reflecting boundary. When the flexible knives are moving, it produces large deformation which influences the flow field. So the fluid-solid coupling is considered, and the air is given as the ALE model, so that Arbitrarily Lagrange-Euler algorithm is used [8, 17-18].

Before setting the speed of the knife rollers, the speed of the knife rollers is test. The result shows that, the motor's rated speed is 5000 r/min, when fully loaded; the maximum speed is 3000 r/min, so the main knife roller's speed is set to be 3000 r/min. The transmission efficiency of the drive belt is 93.3%, so the driven knife roller's speed is 2800 r/min. The speed curves of the two rollers are defined respectively, and the rotation directions of the cutter rollers are respectively set in three situations as follow:

1) Both of the knife roller clockwise motion

2) The main knife roller rotates anticlockwise with the clockwise movement of the driven knife roller

3) The main knife roller rotates clockwise with the anticlockwise movement of the driven knife roller

3. Calculation Results and Analysis to Them

3.1. Velocity Vector Analysis under Different Working Modes

The flexible knife rotates in the middle plane of the knife plate, so the flow field in this plane is analyzed at different modes. As shown in Figure 3, the velocity vector of the flow field is analysed

under three different working modes, when the flexible knife moves to 0.10 s and 0.118 s. When the flexible knife rotates under the third working mode, 4 vortices are formed at the two different times respectively. Eddy current will disturb the flow field, so the maximum flow field disturbance formed by the third working modes.

The number of sugarcane leaves left on the ground is different, and the thickness of the accumulated leaves is about 0~40 mm. The sugarcane leaves which are closer to the left and right outlet are often taken out of the body and not easily to cause entanglement. Therefore, the velocity vector is analyzed at 0~40 mm height from the ground. According to Figure 3, the area of the red box which is close to the ground between the two knife rollers is amplified as that in Figure 4.

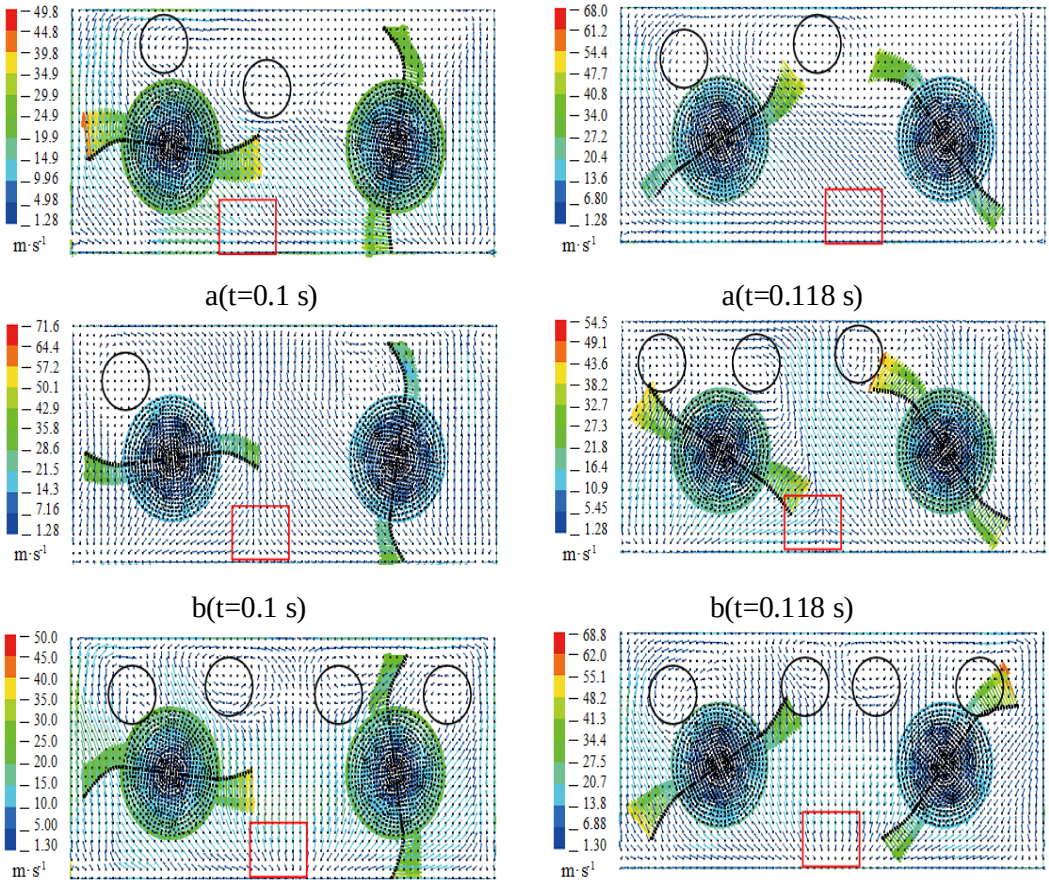

(a)Both of the Knife Roller Clockwise Motion

(b) The main knife roller rotates anticlockwise with the clockwise movement of the driven knife roller

(c) The main knife roller rotates clockwise with the anticlockwise movement of the driven knife roller

Figure 3. Velocity Vector

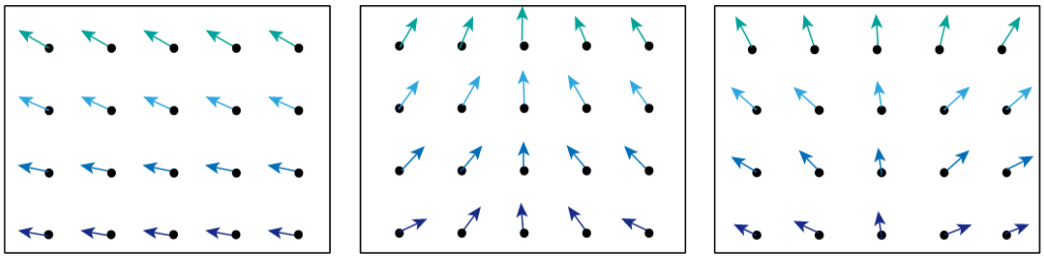

(a) Both of the knife roller clockwise motion

(b) The main knife roller rotates anticlockwise with the clockwise movement of the driven knife roller
(c) The main knife roller rotates clockwise with the anticlockwise movement of the driven knife roller

Figure 4. Speed Vector Local Large Map

The result shows that: With the same direction clockwise rotation, the velocity direction of the region is above the left, and the angle is changed in the range of 10 ~30 degrees. The angle and the height have an increasing function relationship, the greater the height, the larger the angle. When the main knife roller rotates anti-clockwise with the driven knife roller clockwise rotation, the angle change is in the range of about 20 ~90 degrees, the velocity vector direction near the side of the main knife roller is inclined to the right, and the other side velocity vector is inclined to the left. Meanwhile, the velocity vector is basically vertical between of the two knife rollers, equivalent to the Y direction. When the main knife roller rotates clockwise with the driven knife roller anti-clockwise rotation, the speed vector is changed in the range of about 30 ~90 degrees. The velocity vector direction near the side of the main knife roller is inclined to the left, and the other side velocity vector direction is inclined to the right. The direction of velocity vector is exactly opposite to the second working methods, and the middle position is basically the same, which is vertical upward. According to the above analysis, the third working mode is more likely to cause disturbance in the flow field, and the direction of velocity vector in the middle region is more likely to cause sugarcane leaves to be swirled.

3.2. Analysis to the Velocity of Different Height

In order to discuss the problem further, 4 different height's velocities were analyzed respectively. The distance from the ground is 10mm, 20mm, 30mm and 40mm, every height in the horizontal direction is taken at the 10mm distance respectively, 30 points are taken on every line, so 120 nodes are obtained on 4 heights. As shown in Figure 5, the speed of every node is analyzed. Because the vertical direction speed will greatly influence the blowing of the sugarcane leaves, the Y direction speed of every node is extracted in the whole motion process of the system respectively. And then, the maximum speed of every node in the direction of Y in the movement process is found.

According to the previous analysis, the third working mode is easily caused by the flow field disturbance and the blowing of the sugarcane leaves. Therefore, only the two modes are analyzed: both of the knife rollers rotate at the same clockwise direction, and the main roller anti-clockwise rotates with the driven knife clockwise rotation.

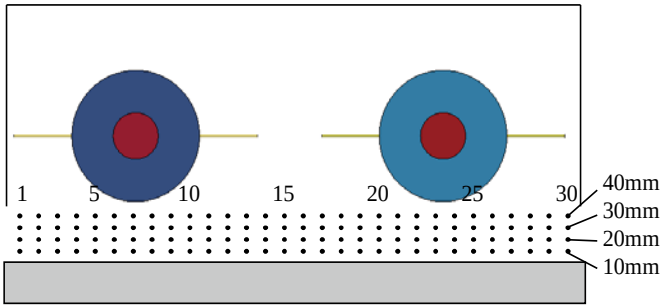

Figure 5. Key-point Position

In order to describe the maximum velocity change at the same height and position more clearly, Gauss function is applied to fitting the data points. The Gauss function fitting equation is as follows:

$$v_y = y_0 + k\, e^{-2\left[(x-a)/b\right]^2} \tag{3}$$

Two different working modes and four different height conditions correspond to eight sets of data. Every group of data is fitted by Gauss. The coefficients in the fitting equation are shown in Table 2:

Table 2. The Coefficient Value

Height	Working mode	y_0	k	a	b
10mm	1	0.744	26.676	18.510	5.680
	2	4.213	43.623	15.856	6.866
20mm	1	1.201	27.684	15.384	10.394
	2	3.144	44.655	15.578	6.487
30mm	1	3.137	44.734	15.567	6.495
	2	0.106	27.932	14.988	10.304
40mm	1	12.649	29.056	2.142	1.072
	2	0.004	51.198	15.646	7.615

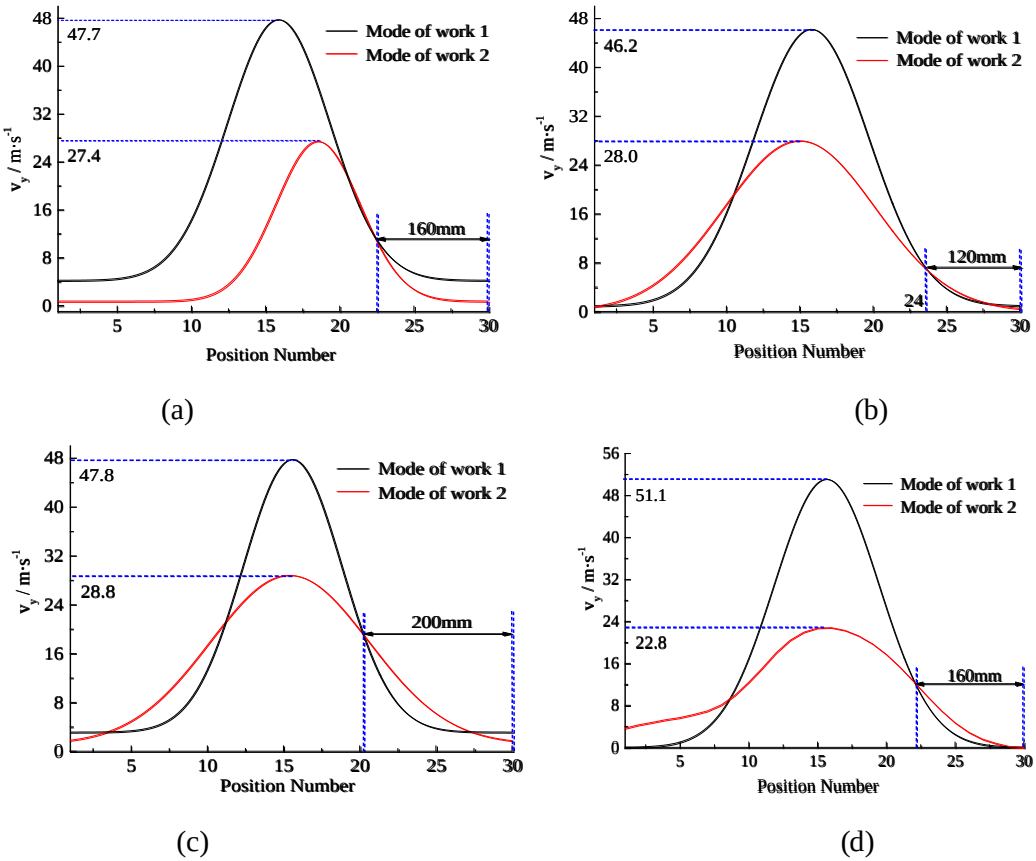

(a) (b)

(c) (d)

(a)10mm (b)20mm (c) 30mm (d) 40mm

Figure 6. Maximum Velocity Variation in Y Direction at Different Positions

As shown in Figure 6, the working mode 1 is the anti-clockwise rotation of the main knife roller with the clockwise rotation of the driven knife roller, and the working mode 2 is the clockwise rotation of the two rollers at the same time. At first, the fitting curve shows that the maximum velocity of the

same height is different from left to right in the whole period. The speed near the outlet of the left and right sides is smaller, and the speed of the middle position between the two knife rollers is the largest, the reason is that the rotation of the flexible knife causes the superposition of the velocity in the middle of the part.

Secondly, in the right side which is near the outlet of the air outlet, the maximum speed of the Y direction is close in the two working modes at the same height, but there is a large difference in the middle area. The superposition of the self-excited wind field caused by the anti-clockwise rotation of the main knife roller with the driven knife roller clockwise rotation is obvious, and the difference is large compared with the clockwise rotation of the two knife rollers.

The maximum speed is found at every height, as shown in Table 3. It is obvious that the maximum speed of the Y direction increases with the height increasing in the 10~30mm under the working mode 1; and the velocity increases with the height increasing in the 20~40mm under the working mode 2. In addition, at the same height, the maximum speed of the Y direction produced under the working mode 1 is greater, the maximum velocity is more than 50m/s when the height is in 40mm, and the difference between the two is up to 55.4%.

Combined with the above analysis, it is found that the working mode 2 is more beneficial than the working mode 1 to reduce the flow field in the body and reduce the effect of blowing and winding of the sugarcane leaves.

Table3. Maximum Velocity of Y Direction m/s

	Different heights (mm)			
	10mm	20mm	30mm	40mm
The working mode 1	47.7	46.2	47.8	51.1
The working mode 2	27.4	28.0	28.8	22.8
The ifference value	42.5%	39.4%	39.7%	55.4%

Table4. Results of Wind Speed m/s

	Different heights (mm)			
	10mm	20mm	30mm	40mm
Left outlet	1.974	3.137	3.432	3.928
Middle position	0.766	0.790	0.958	1.024
Left outlet	-1.235	-1.289	-1.35	-1.367

4. Test Verification and Analysis

4.1. Wind Speed Test

To verify the Modeling and the simulation result, the wind speed measurement of the returning machine is carried out. The test principle is shown in Figure 7.

The velocity is measured under both of the rollers clockwise rotation. The rotational speed is in accordance with the simulation parameters, and the GM8903 hot wire anemometer is selected to measure the wind speed of each key point. Due to the limitation of the installation position of the dome, the wind speed can only be measured under the dome and near the ground. 3 measurement positions are selected; the positions are the left, the middle and the right. Four points are taken at the height of 10mm, 20mm, 30mm and 40mm respectively, in the vertical direction of every position. A total of 12 points are measured. In order to improve the accuracy of measurement, the test was repeated 3 times at every position, and the average value was obtained. The test device gets a set of data every 0.5s, it is equivalent to the average speed of a certain position in every 0.5s. The results of the test are shown in Table 4:

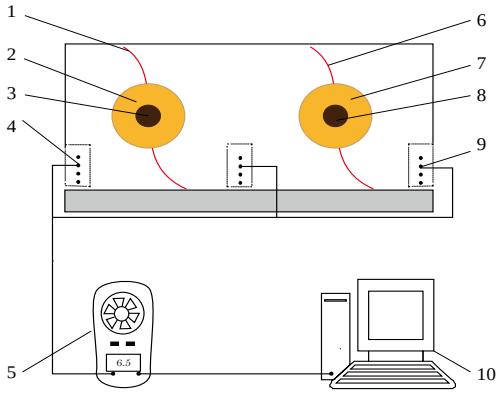

1.№1 flexible knife 2.The main knife roller 3.№1 knife dish 4.№1 test point 5.Anemometer 6.№2 flexible knife 7.The driven knife roller 8.№2 knife dish 9. №2 test point 10. Analysis software

Figure 7. Experimental Schematic Diagram

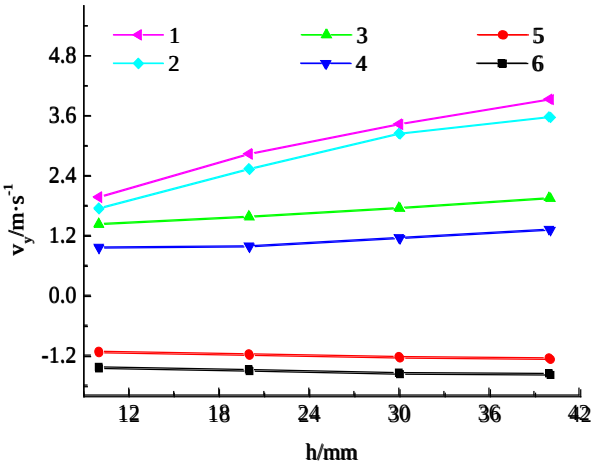

1.Left simulation value 2.Left test value 3.Middle simulation value 4.Middle test value 5.Right simulation value 6.Right test value

Figure 8. Test Value and Simulation Value

Compared with the simulation value, the experimental values of the Y direction of the average wind speed are shown in Figure 8:

The results show that, when the two knife rollers rotate clockwise at the same time, the change trend of the test wind speed is the same as the simulation analysis's result, and it increases with the increase of the height. The test value of the wind speed in each position is close to the simulation value. The maximum gap appears at the middle distance of the ground 20mm positions. The difference between the velocity simulation value and the test value is 17.7%, which may cause certain disturbance to the internal flow field of the anemometer, the instrument itself measure also produces certain deviation, and the deviation is less than 20%, it is in the acceptable range. So the Modeling and the simulation are all reliable.

4.2. High Speed-photography Test

In order to further prove that the both of the knife rollers clockwise movement can reduce the winding of sugarcane leaves, the high-speed photography is carried out to analyze the motion law of sugarcane leaves in the internal flow field.

4.2.1. Experimental Material

The sugarcane leaves were gotten from HEIPI sugarcane variety at Panyu, Guangzhou, China. The harvest time was February in 2018. The leaves of the sugarcane leaves were complete and no breakage, the total length of the leaf (including the leaf sheath) was 80~150 mm.

4.2.2. Experimental Equipment

The main equipment for the high-speed photography test is the returning machine, high-speed camera, flash lamp and computer. The field test is shown in Figure 9. The high-speed photography equipment is M/R/LC110 high-speed camera; the shooting rate is set to 500 frames / sec in the test. In order to avoid the problem of unclear shooting caused by insufficient internal light, two flash lamps are placed near the returning machine. It is equipped with a notebook computer with PCC 2.6.749.0 program. In the experiment, the yellow wire is connected to the computer to realize data transmission. The related parameters of the high-speed camera can be adjusted by the computer, and the results are post-processed.

1. Dome 2. Flash lamp 3. Power cord 4. Network line 5. Returning mechine 6. High-speed camera 7. Computer

Figure 9. High Speed Photography Field Test Chart

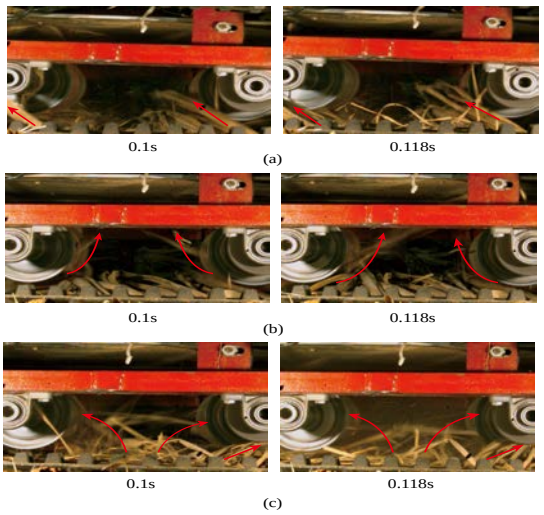

(a) Both of the knife roller clockwise motion (b) The main knife roller rotates anticlockwise with the clockwise movement of the driven knife roller (c) The main knife roller rotates clockwise with the anticlockwise movement of the driven knife roller

Figure10. The Movement State of Sugarcane Leaves under Different Working Conditions

4.2.3. Test Method

On the clean and flat ground, there is a regular flat layer of tested sugarcane leaves in parallel direction with the knife roller, start the sugarcane leaf returning machine and drive it to the ground covered with sugarcane leaves. The flash lamp and the high-speed camera are placed on the same side of the caterpillar track and have a certain sharp angle with it. It ensures that the flow field is light enough and layout of the high-speed camera to meet the requirements of the test area. In accordance with the simulation test, high speed photography tests are carried out under the three different working modes. The speed of the main knife roller is 3000 r/min.

4.2.4. Test Results and Analysis to Them

The results at 0.1s and 0.118s were selected for analysis under different working modes. The motions of the sugarcane leaves are shown in Figure 10.

When the two knife rollers rotate clockwise at the same direction, the sugarcane leaves on the left of the main knife roller can be discharged along the left side; the sugarcane leaves are flying in the middle area of the two knife rollers, Flexible knives further attack and cut the flying sugarcane leaves during the course of rotation, it doesn't the lead sugarcane leaves to twine the knife roller. When the main knife roller rotates clockwise with the driven knife roller anti-clockwise rotation, the sugarcane leaves gather in the middle area. After a period of time, the sugarcane leaves twist the knife rollers. When the main knife roller rotates anti-clockwise with the driven knife roller clockwise rotation, the movement of the sugarcane leaves in the middle of the two knife rollers is more and more disorderly, and there is a tendency to move to the two knife rollers respectively. At the end of the test, there are more sugarcane leaves on the knife rollers.

It shows that the results of high-speed photography coincide with the simulation movement of sugarcane leaves in the sugarcane leaf returning machine, and further proves that the same clockwise movement is beneficial to reduce the problem of winding caused by the blowing of sugarcane leaves.

5. Conclusion

1) Due to the influence of the self-excited wind field caused by the flexible knife on both sides, the internal flow field will produce certain eddy current in the three different working modes; it will cause the flow field to have a turbulent motion. When the main knife roller rotates clockwise with the driven knife roller anticlockwise rotation, there are more turbulent motions.

2) On the basis of the maximum velocity analysis in Y direction, the maximum velocity distribution at the same height from left to right shows a trend of first increase and then decrease. The speed of the two sides near the outlet is small, the speed of the middle area is large, and the peak appears in the middle position. When the main knife roller is revolving anti-clockwise with the driven knife roller clockwise rotation, the Y direction maximum speed in the middle is higher than both of the two rollers movement as the same clockwise rotation. The difference of them is up to 55.4%.

3) The Y direction velocity of three different positions is tested under the two knife rollers in the same clockwise movement. The test results are close to the simulation results. The maximum difference is 17.7%; it is in the acceptable range. The test verifies the accuracy and the reliability of the Modeling and the simulation results.

4) The high-speed photography test is consistent with the simulation results, it verifies the accuracy of the simulation results, and proves that the working mode of the same direction is beneficial to reduce the problem of blowing and winding of sugarcane leaves.

In summary, when the machine works, it is better to choose the working mode of the two knife rollers clockwise rotation, it is beneficial to reduce the blowing of the sugarcane leaves and reduce the winding of the sugarcane leaves as much as possible. This paper provides a reference for further optimization of the flow field in future.

6. Acknowledgement

Subject was supported by the Fund for the Science and Technology Program of Guangzhou (№. 201704020022).

*Corresponding author: Yuxing Wang

7. Reference

[1] Patcharaporn Pongpat, Shabbir H. Gheewala and Thapat Silalertruksa. 2017. An assessment of harvesting practices of sugarcane in the central region of Thailand, *Journal of Cleaner Production*, vol 142, pp 1138-1147.

[2] Jian Yang, Zhaoxin Liang, Jianlin Mo, Yueqian Jin and Meiying Gu. 2005. Vibration simulation of 3SY-140 sugarcane leaf-breaker. *Transactions of the Chinese Society for Agricultural Machinery*, vol 36, No11, pp74-77.

[3] Ming Li, Jinli Wang, Yiguo Deng, Hui Huang and Jin Zhang. 2008. Structural design and experiments on sugarcane leaf shattering and returning machine. *Transactions of the Chinese Society of Agricultural Engineering*, vol 24, No 2, pp121-126.

[4] Hirth A, Haufe A and Oluvsson L. 2007. Airbag simulation with LS-DYNA past - present - future. *Cheminform*, vol 24, No 9, pp394-395.

[5] Escalona J L. 2017. An arbitrary Lagrangian–Eulerian discretization method for modeling and simulation of reeving systems in multibody dynamics. *Mechanism & Machine Theory*, vol 112, pp1-21.

[6] Nassiri A and Kinsey B. 2016. Numerical studies on high-velocity impact welding: smoothed particle hydrodynamics (SPH) and arbitrary Lagrangian-Eulerian (ALE). *Journal of Manufacturing Processes*. Vol 24, part 2, pp376-381.

[7] He Jia, Wei Rong and Guoliang Chen. 2010. The simulation of parachute inflation process based on LS-DYNA software. *Spacecraft Environment Engineering*, vol 27, No 3, pp367-373.

[8] Helenbrook B T and Hrdina J. 2018. High-order adaptive arbitrary-Lagrangian-Eulerian (ALE) simulations of solidification. *Computers & Fluids*, vol167, pp40-50.

[9] Sanbin Lu, Liping Dong, Guang Chen, Junyuan Zhang and Zhichao Yang. 2009. Numerical simulation of curtain airbag deployment based on arbitrary lagrangian - eulerian algorithm. *Automotive Engineering*, vol 31, No 12, pp1158-1161.

[10] Hongxin Liu, Xiaomeng Xu, Junxiao Liu and Chen Wang. 2016. Working characteristics of vertical shallow-basin type seed-metering device based on high-speed photography and virtual simulation. *Transactions of the Chinese Society of Agricultural Engineering*, vol 32, No 2, pp13-19.

[11] He Xing, Ying Zang, Xiaoman Cao, Zaiman Wang and Xiwen Luo. 2015. Experiment and analysis of dropping trajectory on rice pneumatic metering device. *Transactions of the Chinese Society of Agricultural Engineering*, vol 31, No 12, pp 23-30.

[12] Zhichao Hu, Bing Wang, Zhaoyang Yu, Baoliang Peng, Yanhua Zhang and Lvke Tan. 2017. Design and test of semi-feeding test-bed for peanut pod picking. *Transactions of the Chinese Society of Agricultural Engineering*, vol 33, No 17, pp42-50.

[13] Liqing Chen, Dong Zhang and Wuwei Chen. 2014. Numerical simulation and test on two-phase flow inside shell of transfer case based on fluid-structure interaction. *Transactions of the Chinese Society of Agricultural Engineerin*, vol 30, No 4, pp 54-61.

[14] Xiangwei Mou,Yinggang Ou and Hao Wu.2012. Damage of sugarcane leaf sheath under action of elastic leaf-stripping elements based on high-speed photography. *Transactions of the Chinese Society for Agricultural Machinery*, vol 43, No 2, pp85-89.

[15] Xinping Li, Yuli Ma, Lianxing Gao. 2009. High-speed photograph analysis on threshing process of corn seed. *Transactions of the Chinese Society for Agricultural Machinery*, vol 40, No 11, pp46-49.

[16] Shenchang Huang, Wang Yang, Jian Yang and lei Liang. 2018. Study on finite element modeling method of sugarcane stalk-sugarcane leaf system. *Journal of Agricultural Mechanization Research*, vol 40, No 6, pp19-23.

[17] Waltz J and Bakosi J. 2018. A coupled ALE-AMR method for shock hydrodynamics. *Computers & Fluids*, vol 167, pp357-371.

[18] Sean Mauch, Dan Meirona, Raul Radovitzky and Ravi Samtaney. 2003. Coupled Eulerian-Lagrangian simulations using a level set method. *Computational Fluid and Solid Mechanics 2003*. Proceedings Second MIT Conference on Compurational Fluid and Solid Mechanics, June 17–20, 2003, pp1448-1453.